

# Numerical Simulation Study on Influencing Factors and Response Patterns of Loop Source Semi-Airborne Transient Electromagnetic

Tuanbin Liao<sup>1</sup>, Guoqiang Zhang<sup>2</sup>, Bingbing Chen<sup>3</sup>, Lizhi Du<sup>1,\*</sup>

<sup>1</sup>College of Construction Engineering, Jilin University, Changchun 130026, China

<sup>2</sup>Jilin Water Resource and Hydropower Consultative Company of P. R. China, Changchun 130012, China

<sup>3</sup>College of Construction Engineering, Jilin University, Changchun 130026, China

\*Correspondence Author

**Abstract:** *Semi-airborne transient electromagnetic method (SATEM), as an efficient geophysical exploration technique, combines the deep detection capability of ground-based transient electromagnetic methods with the high-efficiency data acquisition advantages of airborne electromagnetic methods. It is particularly suitable for areas with complex terrain, such as lakes, swamps, and mountainous regions. This paper focuses on loop-source SATEM as the research subject. Based on a one-dimensional forward modeling approach, we investigate the influence mechanisms of key factors—including transmitter current intensity, loop-source size, formation resistivity, and flight altitude—on transient electromagnetic signals. The study employs the Finite Volume Method for numerical simulation of a homogeneous half-space model. By constructing multiple sets of comparative experiments, we quantitatively analyze the spatiotemporal evolution characteristics of vertical magnetic field response curves under different parameter combinations. The results indicate that optimal signals can be acquired when the aircraft flies at lower altitudes, transmitter current intensity is maximized as much as possible, exploration is conducted in regions of low formation resistivity, and the most reasonable transmitter side length is selected.*

**Keywords:** Semi-airborne transient electromagnetic, Loop source, Numerical simulation, One-dimensional forward modeling.

## 1. Introduction

The semi-airborne transient electromagnetic method (SATEM) is an electromagnetic exploration technique that involves transmitting high-power primary electromagnetic signals from the ground and measuring the secondary electromagnetic fields—generated by induced eddy currents in subsurface media—using airborne receivers during the primary field off-time. Substantial research on SATEM has been conducted by scholars both domestically and internationally.

Originally proposed by Nabighian in 1988, SATEM provided the foundational theoretical framework. Early systems include TURAIR, FLAIRTEM, Terra Air, and GREATEM. TURAIR operates in the frequency domain, similar to Airborne Electromagnetic (AEM) systems. FLAIRTEM employs a large ground loop transmitter with an airborne receiver, Elliott et al successfully utilized this system to explore geological features beneath conductive overburden in arid regions (Elliott et al., 1996). Fugro developed the Terra Air semi-airborne system in 1997, which uses a large ground loop source as the transmitter and a towed airborne receiver featuring full-time-domain continuous recording technology. This innovation enabled real-time synchronous data processing during acquisition. Smith applied this system to explore massive sulfide deposits, demonstrating that SATEM data exhibits a signal-to-noise ratio intermediate between ground-based and airborne TEM systems (Smith et al., 2001). GREATEM is a SATEM system designed for deep structure detection. Mogi et al first adapted it for helicopter deployment in 1998, conducting field tests in geothermal areas and highlighting its advantages for imaging deeper structures and resolving resistivity responses at depths of 100–200 meters (Mogi et al., 1998). In 2009, they completed volcanic subsurface structure surveys at Mount Bandai, northeastern

Japan, proving its theoretical detection depth could reach 800 meters under specific conditions (Mogi et al., 2009). From 2013 to 2014, Ito et al employed the GREATEM system with a 3-km long-wire source to explore the deep resistivity structure of Aso Volcano. Comparisons with ground TEM data confirmed feasibility, achieving an exploration depth of 800 meters (Ito et al., 2014). Research on SATEM systems in China began relatively later. Yanju Ji et al. from Jilin University pioneered its study in China by using an unmanned airship as a flight platform for data acquisition within the research project "Development of Time-Domain Ground-Air Electromagnetic Detection Instrumentation," based on prior numerical simulations and field tests (Ji et al., 2013). Jun Lin developed a semi-airborne time-frequency co-detection system and conducted extensive related research (Lin et al., 2021).

Despite demonstrating unique advantages in specific scenarios, these SATEM systems face common practical challenges. Furthermore, systematic studies on optimizing key parameters—such as transmitter current intensity, loop size, and flight altitude—remain scarce. Research on identifying the optimal survey area for loop-source SATEM is particularly limited. Addressing this gap, this study employs multi-parameter coupling analysis to define principles for optimal survey area selection in loop-source SATEM. We propose an exploration strategy prioritizing "low-altitude flight, high transmitter current, small loop sources, and low-resistivity target zones." This framework provides theoretical support for the engineering design and data interpretation of SATEM systems in complex terrains.

## 2. Principle of Detection Technology

The semi-airborne transient electromagnetic detection system comprises a ground-based transmitting unit and an air-based

receiving module as shown in Figure 1. The ground unit establishes a primary field source by deploying a rectangular transmitting loop, using a bipolar square-wave pulse current to excite the subsurface medium and generate a transient electromagnetic field. The aerial platform employs a multi-rotor UAV carrying a receiving coil, executing variable-altitude spiral flight paths based on a pre-defined digital elevation model to collect electromagnetic response data. This architecture implements an air-ground collaborative observation mode, achieving spatial decoupling of electromagnetic energy radiation and signal reception.

Based on Faraday's law of electromagnetic induction, the step-off current pulse (magnitude: 1–500 A) generated by the ground-based transmitting loop induces an eddy current field in the subsurface medium. Following the termination of the transmission current, the induced eddy currents in the conductive subsurface medium decay according to the diffusion equation, forming observable secondary field signals. By acquiring time-domain electromagnetic responses during the current-off period ( $10^{-6}$ – $10^{-3}$  s), an apparent resistivity-time depth model can be established.

$$\rho_s(t) = \frac{\mu_0}{4\pi t} \left( \frac{m \cdot I}{V(t)} \right)^{2/3} \quad (1)$$

Within the equation,  $m$  represents the transmitter magnetic moment,  $I$  denotes the excitation current, and  $V(t)$  is the normalized decay voltage. This model reveals the quantitative relationship between the electrical properties of the subsurface media and the characteristics of the electromagnetic decay.

In the field of mineral resource exploration, this technology has been successfully applied to the detection of deep-seated concealed ore bodies. Field measurements demonstrate a vertical resolution better than 15 meters for sulfide-type mineral deposits. For engineering geological surveys, the identification rate of geohazard features—such as karst collapse zones and fault fracture zones—reaches 92%, significantly outperforming conventional geophysical methods. With the integration of intelligent inversion algorithms, semi-airborne transient electromagnetic methods are progressively advancing toward multi-parameter quantitative interpretation, demonstrating strategic significance in deep earth resource exploration.

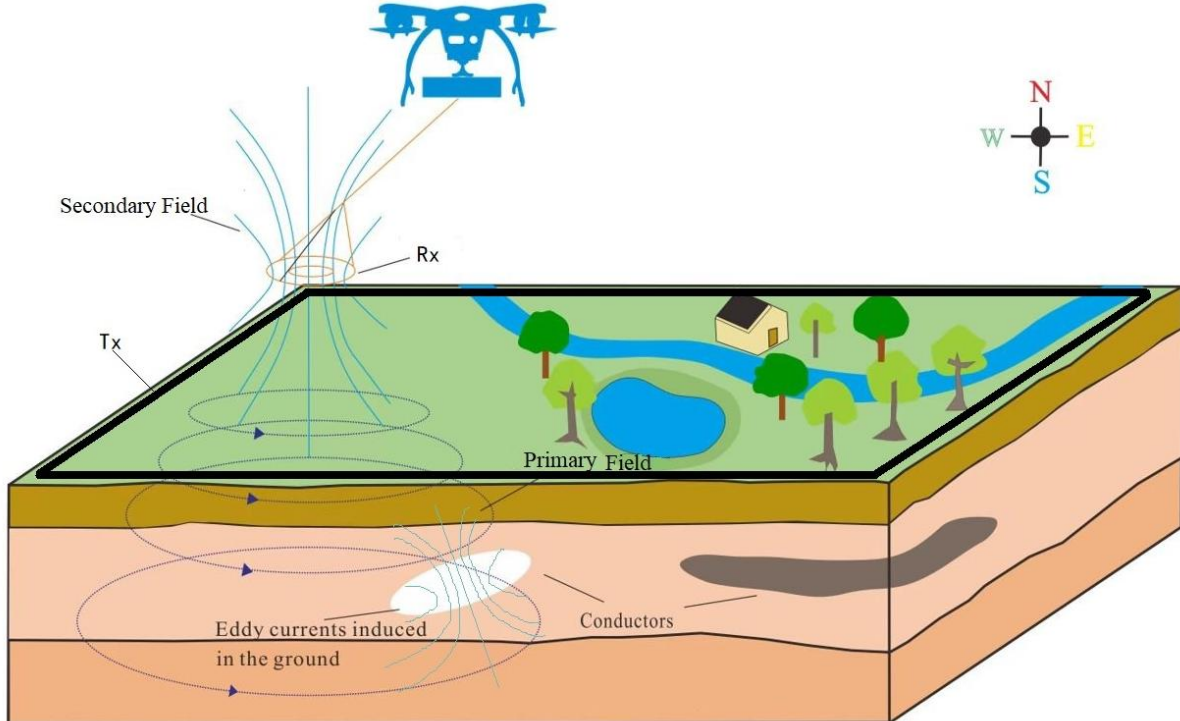


Figure 1: Schematic diagram of SATEM detection

### 3. Methodology

The theoretical basis for semi-airborne transient electromagnetic exploration is grounded in Maxwell's equations. In the time domain, Maxwell's equations take the following form:

$$\nabla \times \mathbf{e} = -\frac{\partial \mathbf{b}}{\partial t} \quad (2)$$

$$\nabla \times \mathbf{h} = \mathbf{j} + \frac{\partial \mathbf{d}}{\partial t} \quad (3)$$

$$\nabla \mathbf{b} = 0 \quad (4)$$

$$\nabla \mathbf{d} = \rho \quad (5)$$

Where  $\mathbf{j}$  is the current density and  $\rho$  is the charge density.

$$\mathbf{E}_r = \mathbf{E}_z = 0, \mathbf{E}_\varphi = -i\omega\mu \frac{\partial \mathbf{A}_z^*}{\partial r}, \mathbf{H}_r = \frac{\partial^2 \mathbf{A}_z^*}{\partial^2 r}, \mathbf{H}_z = k^2 \mathbf{A}_z^* + \frac{\partial^2 \mathbf{A}_z^*}{\partial^2 z}, \mathbf{H}_\varphi = 0 \quad (6)$$

The closed-form analytical solution for  $\mathbf{A}$  in the region above the  $n$ -layered medium interface is:

$$\mathbf{A}_z^* = \frac{M}{4\pi} \int_0^\infty \left( e^{-m|z|} + \frac{mR_n^* - m_1}{mR_n^* + m_1} e^{m|z|} \right) J_0(mr) dm \quad (7)$$

The total electric field generated by the magnetic dipole current above the layered ground is:

electric field tangential direction:

$$E_\varphi = \frac{i\omega M}{4\pi} \int_0^\infty m \left( e^{-m|z|} + \frac{mR_n^* - m_1}{mR_n^* + m_1} e^{m|z|} \right) J_1(mr) dm \quad (8)$$

Magnetic field radial direction:

$$H_r = \frac{M}{4\pi} \int_0^\infty m^2 \left( e^{-m|z|} - \frac{mR_n^* - m_1}{mR_n^* + m_1} e^{m|z|} \right) J_0(mr) dm \quad (9)$$

Magnetic field vertical direction:

$$H_z = \frac{M}{4\pi} \int_0^\infty m^2 \left( e^{-m|z|} + \frac{mR_n^* - m_1}{mR_n^* + m_1} e^{m|z|} \right) J_0(mr) dm \quad (10)$$

The relationship between the induced electromotive force and the vertical magnetic field is:

$$V = -\frac{\mu \partial H_z}{\partial t} \cdot S \quad (11)$$

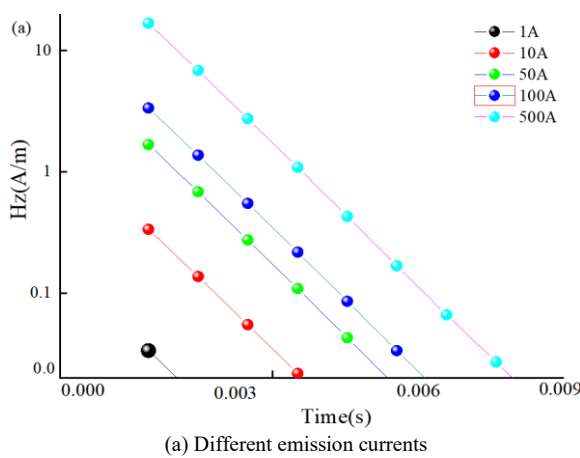
From this it can be obtained:

$$H_z = -\frac{1}{iw\mu} \frac{V}{S} \quad (12)$$

## 4. Test Results and Analysis

### 4.1 Response Pattern of Vertical Induced Magnetic Field Under Different Emission Currents

To investigate the influence mechanism of excitation current parameters on transient electromagnetic response characteristics, a geological-geophysical forward model was established for uniform half-space scenarios. This model simulates the spatial distribution patterns of vertical magnetic field components in SATEM systems, with host rock resistivity set at  $100 \Omega \cdot \text{m}$ , transmitter loop dimensions of  $100 \times 100 \text{ m}$ , base excitation current of 1 A, and frequency of 25 Hz. Based on observations at spatial coordinate point  $(0, 0, -30)$ , forward modeling calculations were performed to determine the vertical component amplitude response of induced fields under multi-level excitation currents (stepwise variation from 1A to 500A). This enables systematic analysis of current-intensity dependence characteristics for semi-airborne TEM fields in uniform half-space, as shown in Figure 2.



(a) Different emission currents

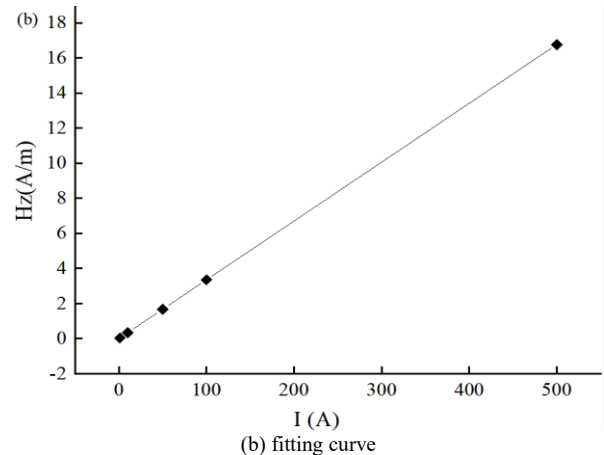


**Figure 2:** Vertical component response patterns of the SATEM system in uniform half-space with varying emission currents

Analysis of observational data reveals in Figure 2a: under constant flight altitude conditions, excitation current intensity demonstrates a significant positive correlation with induced field amplitude. Increasing transmitter current effectively enhances signal strength, particularly in low-resistivity formations ( $\rho < 100 \Omega \cdot \text{m}$ ), while transient response waveforms exhibit high similarity across different current levels. Theoretical verification further demonstrates in Figure 2b: The amplitude of the vertical magnetic field component shows strict linear growth with increasing current intensity, following the proportionality principle derived from Maxwell's equations. Based on these findings, we recommend optimizing transmitter power parameters in SATEM survey systems. Enhancing excitation current intensity can acquire induced signals with higher signal-to-noise ratios, thereby significantly improving detection resolution for deep geological targets.

### 4.2 Response Pattern of Vertical Induced Magnetic Field Under Different Transmitting Side Lengths

This study aims to investigate the influence mechanism of transmitter loop geometric dimensions on the vertical magnetic field component response characteristics of the SATEM system in a uniform half-space medium. The parameters of the established geoelectrical model are as follows: medium resistivity uniformly set to  $100 \Omega \cdot \text{m}$ , base transmitter loop of  $100 \times 100 \text{ m}$  square configuration, excitation current intensity of 1 A, operating frequency of 25 Hz, and observation point coordinates at  $(0, 0, -30)$ . The system calculated the amplitude distribution characteristics of the vertical component of the induced magnetic field for transmitter loop side lengths ranging from 20 to 600 m (eight specifications: 20, 50, 100, 200, 300, 400, 500, and 600 m), and plotted the transient electromagnetic response signature spectra as functions of transmitter size under uniform half-space conditions, as shown in Figure 3.

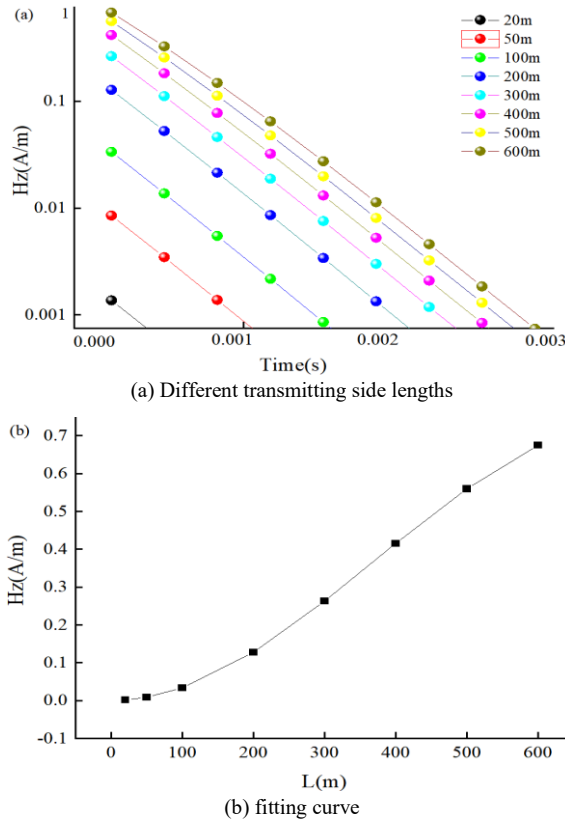


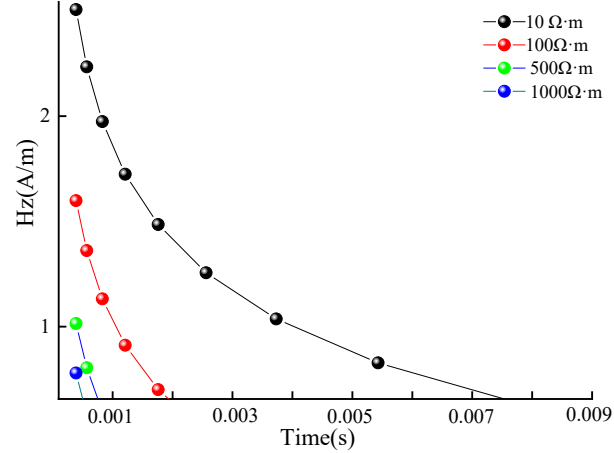
**Figure 3:** Vertical component response patterns of the SATEM system in uniform half-space with varying transmitter side lengths

According to the observational data in Figure 3a, within the uniform half-space model featuring a 1 A transmitter current and  $100 \Omega\cdot\text{m}$  medium resistivity, the induced magnetic field strength demonstrates a significant enhancement trend with increasing transmitter loop geometric dimensions. Figure 3b further reveals: during the expansion of transmitter size from 20 m to 200 m, the growth gradient of early-time transient electromagnetic response amplitudes remains relatively gradual; within the 200–500 m scale range, the induced field amplitude exhibits an approximately linear growth relationship with loop size; beyond 500 m, the response enhancement trend markedly attenuates, indicating gradual reduction in electromagnetic source coupling efficiency with geometric expansion. Specifically, while increasing loop side length expands detection coverage, its gain effect on electromagnetic response reaches a critical threshold (side length  $\approx 500$  m), beyond which signal amplification tends toward saturation. These findings collectively demonstrate that optimal transmitter loop sizing in semi-airborne transient electromagnetic exploration must comprehensively consider critical parameters including target occurrence depth, host rock electrical properties, and excitation current intensity—rather than pursuing maximum geometric dimensions alone.

#### 4.3 Response Patterns of Vertical Induced Magnetic Fields Under Varying Subsurface Resistivity

This study aims to reveal the response mechanism of formation conductivity parameters to the vertical magnetic field component of the SATEM system within a uniform half-space medium. The established geoelectrical model employs the following baseline parameters: a  $100 \times 100$  m

square transmitter loop, excitation current of 1 A, operating frequency of 25 Hz, and receiver coordinates at  $(0, 0, -30)$ . The system calculated the amplitude distribution of the vertical component of the induced magnetic field for host rock resistivities ranging from 10 to  $1000 \Omega\cdot\text{m}$  (across four gradients: 10, 100, 500, and  $1000 \Omega\cdot\text{m}$ ), and plotted the transient electromagnetic response signatures for media with varying conductive properties, as shown in Figure 4.



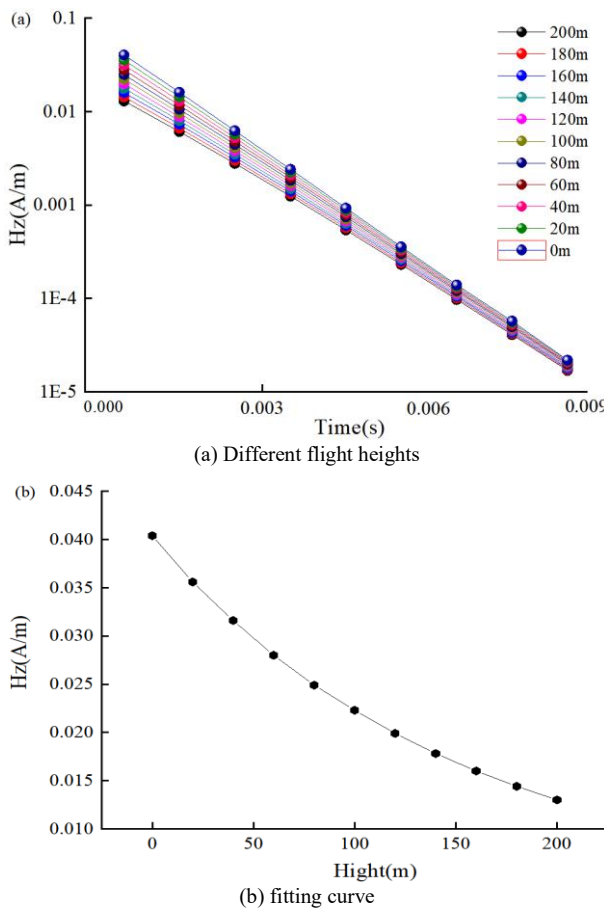
**Figure 4:** Amplitude variation curve of semi-airborne electromagnetic response with different resistivity in uniform semi-infinite space

Figure 4 data demonstrates that within a uniform half-space medium, the induced magnetic field intensity exhibits globally accelerated attenuation with increasing medium resistivity, and this attenuation gradient progressively moderates over time. Specifically: electromagnetic response amplitudes are significantly enhanced for low-resistivity targets ( $10\text{--}100 \Omega\cdot\text{m}$ ), with transient field decay characteristics showing pronounced retardation—indicating slower signal decay rates and more evident late-time response delays in low-resistivity environments, highlighting SATEM's heightened sensitivity to low-resistivity anomalies. Conversely, high-resistivity media ( $500\text{--}1000 \Omega\cdot\text{m}$ ) exhibit sharply reduced induced field amplitudes with rapidly vanishing response curves. This decay disparity originates from the skin effect. Notably, while transient response decay patterns across different resistivity models maintain high similarity, every order-of-magnitude decrease in conductivity parameters systematically delays the onset of late-time responses (as evidenced by curve cluster offsets in Figure 4). This phenomenon confirms the significant sensitivity of the Semi-Airborne Transient Electromagnetic method to variations in medium conductivity.

#### 4.4 Response Patterns of Vertically Induced Magnetic Fields at Different Flight Heights

This study established a standard geological model to investigate the effect of detector height above ground on the vertical magnetic field response characteristics of the SATEM system in an isotropic, homogeneous half-space. The key parameters of the theoretical model were set as follows: the host rock conductivity was fixed at  $100 \Omega\cdot\text{m}$ , the excitation source was a  $100 \text{ m} \times 100 \text{ m}$  rectangular transmitter loop carrying a current of 1 A with a fundamental operating frequency of 25 Hz. Numerical simulations were performed to obtain the vertical component intensity of the induced magnetic field at 11 elevation intervals (20 m spacing),

covering a range from 0 m to 200 m above the ground surface. Based on these results, a characteristic spectrum of the transient field response versus height was generated, as shown in Figure 5.



**Figure 5:** Vertical component response patterns of the SATEM system in uniform half-space with varying flight heights

Figure 5a data demonstrates that flight altitude significantly impacts early-time signals. For every 50 m increase in altitude, the response amplitude attenuates by approximately 30%. However, late-time signals are less affected by altitude variations, indicating that low-altitude flights (<100 m) can significantly enhance data quality. Figure 5b further reveals that the electromagnetic signal follows a nonlinear decay pattern with increasing altitude. The physical origin of this phenomenon lies in the following: compared to ground-based transient electromagnetic systems, the semi-airborne TEM system incorporates an air layer (with a thickness equal to the flight altitude and resistivity approaching infinity) superimposed on the homogeneous half-space model. During the late-time response stage, the electromagnetic signals converge to a steady state regardless of altitude variations.

## 5. Conclusion

(1) The amplitude of the electromagnetic response exhibits a strong positive correlation with transmitter current intensity. Enhancing the transmitter current can effectively boost signal strength, with this effect being particularly pronounced in conductive formations.

(2) Increasing the side length of the transmitter loop expands the investigation coverage area. However, its signal

enhancement effect exhibits a threshold behavior (critical side length  $\approx 500$  m), beyond which the returns diminish significantly. Optimization based on target depth and geological constraints is therefore required.

(3) Subsurface resistivity exhibits an inverse correlation with electromagnetic response magnitude. In conductive environments, the signal decay rate is slower, resulting in more pronounced late-time response delays. This highlights the high sensitivity of SATEM to conductive anomalies.

(4) Flight altitude significantly affects early-time signals, with response amplitude attenuating by approximately 30% per 50 m increase in height. However, late-time signals exhibit minimal sensitivity to altitude variations. This empirical evidence confirms that low-altitude operations (<100 m) substantially enhance data quality.

In summary, via multi-parameter coupling analysis, this paper clarifies the principles for selecting the optimal observation area for loop-source SATEM surveys. It proposes a detection strategy characterized by "low-altitude flight, high transmitter current, small loop sources, and prioritizing low-resistivity target zones." This provides theoretical support for the engineering design and data interpretation of ground-air TEM systems in complex terrains. Future research could further combine three-dimensional modeling and field measurements to validate and enhance the applicability and accuracy of this methodology.

## References

- [1] Elliott P. 1996. New airborne electromagnetic method provides fast deep-target data turnaround[J]. The Leading Edge, 15(4): 309-310.
- [2] Elliott P. 1998. The principles and practice of FLAIRTEM [J]. Exploration Geophysics, 29(2): 58-60.
- [3] Smith R S, Annan A P, Mc G P D. 2001. comparison of data from airborne, semi airborne, and ground electromagnetic systems[J]. Geophysics, 66(5): 1379-1385.
- [4] Mogi T, Tanaka Y, Kusunoki K, et al. 1998. Development of grounded electrical source airborne transient EM(GREATEM)[J]. Exploration Geophysics, 1998, 29(2): 61-64.
- [5] Ito H, K H, Mogi T, et al. 2014. Grounded electrical-source airborne transient electromagnetics (GREATEM) survey of Aso Volcano, Japan[J]. Exploration Geophysics, 45(1):43-48.
- [6] Chen B B. 2018. Research on the Application of Ground-Air Transient Electromagnetic System Based on Loop Source [D]. Jilin University.
- [7] Xiang X B. 2024. Research on Noise Processing of Ground-Air Transient Electromagnetics with Fixed-Source Loop [D]. Kunming University of Science and Technology.
- [8] Ji Y J, Wang Y, Xu J, et al. 2013. Time-domain ground-to-air electromagnetic exploration system for long wire source of unmanned airship and its application [J]. Chinese Journal of Geophysics, 56(11):3640-3650.
- [9] Xu Dingfu. 2024. Analysis of Electromagnetic Responses Excited by Finite-Length Grounded

Conductors in Boreholes within Layered Earth [D].  
Guilin University of Technology.

[10] Zhai Hao. 2024. Research and Application on Transient Electromagnetic Detection Capability of Semi-Airborne Utetheisa Kong [D]. Jilin University.

[11] Han Yu. 2024. One-Dimensional Forward Modeling of Spectral Induced Polarization Considering Pure Induced Polarization Effect and Electromagnetic Coupling Effect [D]. Guilin University of Technology.

[12] Hu Yingcai, Wang Ruiting, Prunus Salicina Xiu. 2023. One-Dimensional Forward Modeling of Transient Electromagnetic Fields for Arbitrarily Oriented Long-Wire Sources [J]. Journal of Engineering Geophysics, 20(06): 796-806.

[13] Wang Yingying. 2023. Numerical Simulation Study of Transient Electromagnetic Responses Based on Utetheisa Kong Gradient [D]. Jilin University.

[14] Qian Weizhou, Chen Hui, Deng Juzhi, et al. 2023. One-Dimensional Forward Modeling and Response Characteristics of Vertical Magnetic Dipole Frequency-Domain Electromagnetic Sounding [J]. Science Technology and Engineering, 23(12): 4958-4964.

[15] Zhang Hui. 2022. One-Dimensional Forward Modeling of Apparent Resistivity for Magnetic Dipole Sources in Layered Media [J]. Energy Technology and Management, 47(05): 183-185.

[16] Zhang Zhenxiong, Yi Guocai, Wang Shixing, et al. 2021. Research on One-Dimensional Forward and Inverse Modeling Technology of Semi-Airborne Utetheisa Kong Transient Electromagnetic Method Based on Minimum Broussonetia Papyrifera Construction Model [J]. Computing Techniques for Geophysical and Geochemical Exploration, 43(03): 352-359.

[17] Zhang Zhenxiong. 2021. Research and Application on One-Dimensional Forward and Inverse Modeling of Long-Wire Source Semi-Airborne Utetheisa Kong Transient Electromagnetic Method [D]. Chengdu University of Technology.

[18] Yin Cheng. 2021. One-Dimensional Forward Modeling of Transient Electromagnetic Method with Rectangular Loop Source [J]. Jilin Water Resources, (02): 9-12.

[19] Tong Xiaozhong, He Ting, Zhao Lifang, et al. 2020. Simulation of One-Dimensional Magnetotelluric Responses Using Chebyshev Spectral Method [J]. Journal of Engineering Geophysics, 17(06): 752-758.

[20] Wei Guangjing, Zhang Yanjun, Meng Fanxing, et al. 2020. Application of One-Dimensional Forward and Inverse Modeling Technology of Controlled Source in Geothermal Exploration [J]. Land and Resources Herald, 17(03): 25-30.